Electrochemistry Communications 115 (2020) 106732

Contents lists available at ScienceDirect

Electrochemistry Communications

journal homepage: www.elsevier.com/locate/elecom

Electrochemistry at the liquid–liquid interface rediscovers interfacial polycondensation of nylon-6,6

Karolina Kowalewska[a], Karolina Sipa[a], Andrzej Leniart[a], Sławomira Skrzypek[a], Lukasz Poltorak[a,*]

[a] Department of Inorganic and Analytical Chemistry, Electroanalysis and Electrochemistry Group, Faculty of Chemistry, University of Lodz, Tamka 12, 91-403 Lodz, Poland

ARTICLE INFO

Keywords:
Interfacial polycondensation
ITIES
Miniaturization
Molecular sieving
Polyamide
Interfacial modification

ABSTRACT

The interfacial polymerization of nylon-6,6 is studied at the polarized liquid–liquid interface. The optimal conditions (concentration of reagents in a biphasic system, pH of the water phase, voltammetric cycling) are used to modify the interface, supported by a microcapillary, giving a platform with molecular sieving properties.

1. Introduction

The beauty of the liquid–liquid interface (LLI) lies in its asymmetric properties, which allow the separation of reagents based on their affinity to one or other of the immiscible solvents. This two-phase system provides a unique environment for the preparation of nano/microstructured materials that are difficult or impossible to prepare using other methodologies. The LLI modification can be performed either *ex situ* (the modifier is added to one of the phases) or *in situ* (interfacial decoration follows an interfacial reaction) [1]. In either case, the modifier remains at the interface as the condition for interfacial free energy reduction has to be met. The numerous examples of the reactions that can occur at the LLI are nicely summarized in an elegant review by Piradashvili et al. [2]. The interfacial polycondensation reactions between diamines and diacid chlorides provide an extremely simple way of producing polyamide at the LLI [3]. This reaction, first reported in 1935, not only found commercial success but is also known as a very nice undergraduate experiment – "the nylon rope trick". Other examples placing synthetic chemistry at the LLI may be achieved with the help of "click chemistry", including copper-catalyzed azide–alkyne reactions (e.g. for glycol nanocapsules entrapping oily core creations [4]) or thiol–ene polyaddition (e.g. for the synthesis of chitosan nanocapsules [5]).

Another property of the LLI, frequently coupled to interfacial modification, is the relative ease of operating on different scales, ranging from macroscopic and planar systems down to configurations based on nanodroplets. When placed in a container, the immiscible liquids simply separate to form a continuous and defect-free layer with dimensions defined by its support. Droplets, in turn, can be produced by means of a high energy supply (e.g. sonication) [6], a membrane-based approach [7] or microfluidics [8]. One of the immiscible liquids can be placed in a confined space such as a single nano/micropore or an array of such pores, giving alternative configurations for LLI studies [9–12]. Finally, the LLI can be enriched by another gas or solid phase, forming a multiphase junction. The latter scenario is especially interesting when solid electrodes are employed. Within such a three-phase junction, interdependent electrochemical and chemical reactions can lead to very localized deposition of materials [13–17].

An electrified LLI or interface between two immiscible electrolyte solutions (ITIES) offers electrochemical control during the interfacial modification process. In this respect, a few scenarios can be considered. In the first, a deposit can be formed upon reaction between reactants separated by the LLI (with either one or both having ionic chemical functionality within their structures) where interfacial transfer can be forced via the application of an external potential difference. This methodology was applied to decorate LLI with silica films after adopting a templated sol-gel process [18–21]. LLI polarization may also be used to create floating films of proteins [22–24] or multi-charged species [25,26] electrochemically adsorbed to the soft junction after complex formation with the hydrophobic ions of the organic phase background electrolyte. Finally, the LLI is an environment where heterogeneous redox reactions can proceed. As such, it can be decorated with metallic NPs via the reduction of metal precursors dissolved in one phase (e.g. chloro complexes of Pt or Pd hosted by the water phase)

* Corresponding author.
E-mail address: lukasz.poltorak@chemia.uni.lodz.pl (L. Poltorak).

https://doi.org/10.1016/j.elecom.2020.106732
Received 24 March 2020; Received in revised form 6 April 2020; Accepted 13 April 2020
Available online 15 April 2020

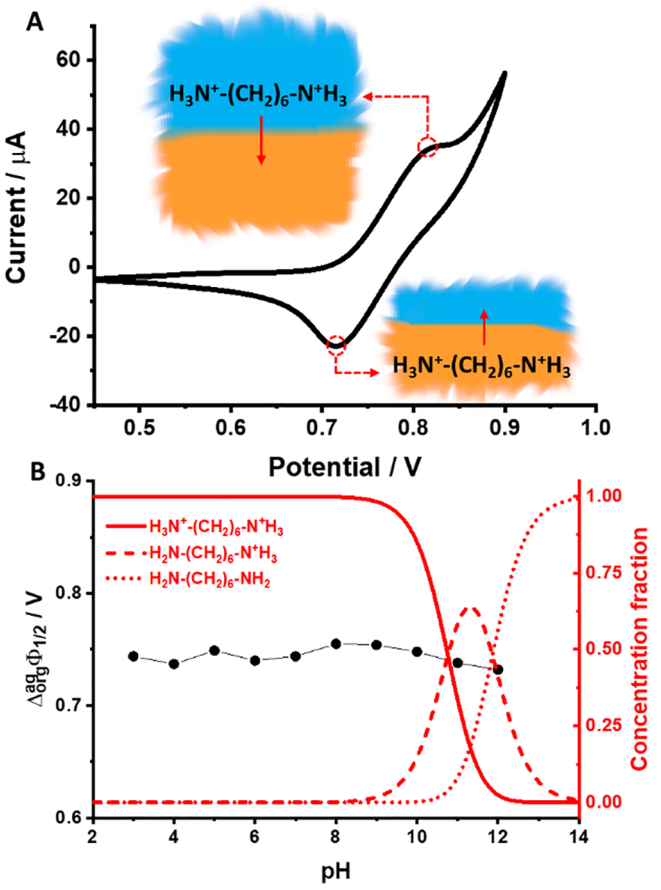

Fig. 1. A Ion transfer voltammogram (ITV) recorded in the presence of 110 μM 1,6-DAH in the water phase (pH ≈ 2, scan rate 10 mV·s^{-1}). The direction of the 1,6-DAH ion transfer is also shown schematically and is attributed to the corresponding signal. **B** The marked points (the line joining them is only a guide for the eye) represent the half-wave potential for the interfacial ion transfer of 1,6-DAH, extracted from voltammograms recorded at different pH values. The red lines represent the distribution diagram of all possible 1,6-DAH species. (For interpretation of the references to colour in this figure legend, the reader is referred to the web version of this article.)

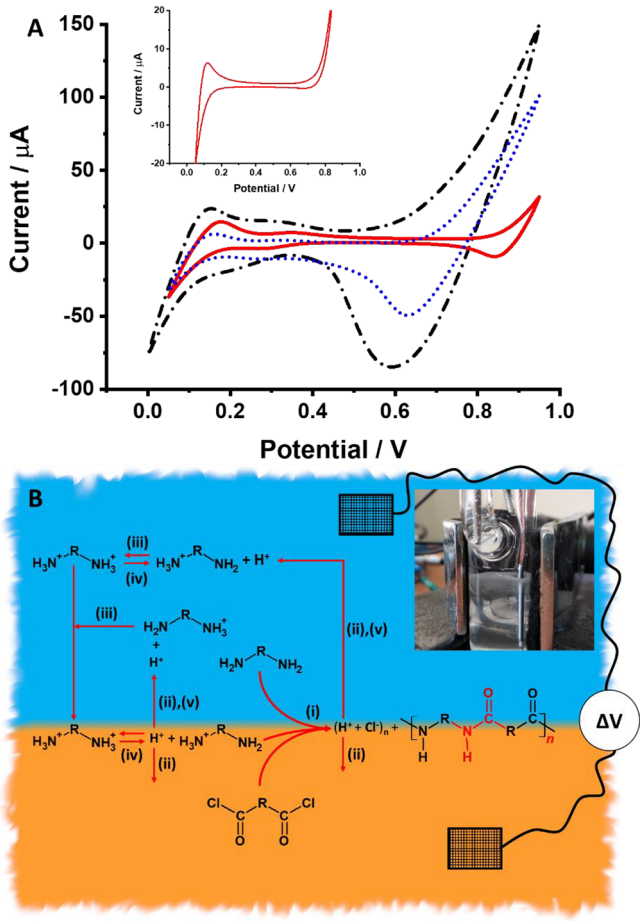

Fig. 2. A ITVs recorded with 5 mM 1,6-DHA in the aqueous phase (dotted blue curve); with 5 mM adipoyl chloride (AC) in the organic phase (solid red curve); and with 5 mM 1,6-DHA in the aqueous phase and 5 mM AC in the organic phase (dot-dash black curve) at a pH equal to 12. The inset shows the voltammogram recorded with 5 mM AC dissolved in the organic phase and the pH of the aqueous phase equal to 2. **B** Proposed mechanism of electrochemically-assisted polyamide formation. A description of the reactions labelled (i) to (v) is given in the text. (For interpretation of the references to colour in this figure legend, the reader is referred to the web version of this article.)

using the electrons from electron donors present in the second phase (e.g. ferrocene derivatives dissolved in the organic solvent) [27–30]. A few examples exist where an electrochemically controlled interfacial electron transfer reaction is used to trigger interfacial polymerization of e.g. polythiophenes [31] or polypyrrole [32,33].

2. Methods and materials

All of the methods, materials and equipment used in this work are described in Section 1 of the electronic Supporting information.

3. Results and discussion

In this work, for the first time, we have used electrochemical control to study nylon-6,6 polycondensation at the polarized water – 1,2-dichloroethane interface. Fig. 1A shows the ion transfer voltammogram (ITV) recorded in the macroscopic electrochemical cell formed upon contacting 110 μM 1,6-diaminohexane (1,6-DAH) dissolved in 10 mM HCl (pH ≈ 2) with 5 mM organic electrolyte solution (for details refer to Supporting information, Section 1.1) dissolved in 1,2-dichloroethane.

Two characteristic signals were recorded and correspond to the interfacial transfer of the charged 1,6-DAH from the aqueous to the organic phase – the positive peak current – and its back transfer from the organic to the aqueous phase, recorded as the negative peak current. The signal originating from the 1,6-DAH appears at around 0.75 V and is partially overlaid with the interfacial transfer of H^+ limiting the potential window on the more positive potential side. Electrochemical characterization of the 1,6-DAH revealed that (i) the corresponding ionic currents can be detected from concentrations as low as 1 μM (see Fig. S1A); (ii) the ratio of the forward and reverse peak current approaches unity, indicating a reversible simple ion-transfer reaction; (iii) the peak-to-peak separation is equal to about 30 mV (within the lower concentration range), which agrees well with the anticipated charge $z = 2$ for pH = 2; (iv) the diffusion coefficient of the 1,6-DAH calculated using the Randles-Sevcik equation is equal to $2.3 \cdot 10^{-6}$ cm^2·s^{-1} and agrees well with the value given in the literature – $1.2 \cdot 10^{-6}$ cm^2·s^{-1} [34] (for details see the Supporting information, Section 2.2). Fig. 1B shows the relation between the half-wave potential of ion transfer for the 1,6-DAH and the pH of the aqueous phase (Britton-Robinson buffer), which is correlated with the fraction of different 1,6-DAH species present in the water phase at different pH values.

The latter data (Fig. 1B in red) were plotted using $pKa_1 = 10.8$ and $pKa_2 = 11.9$ (for details, see Section 2.3 in the Supporting information) [35]. As expected, up to pH 8–9 the potential of 1,6-DAH ion transfer remains largely unaffected as nearly 100% of 1,6-DAH species are fully protonated (each molecule holds two positively charged amine groups –

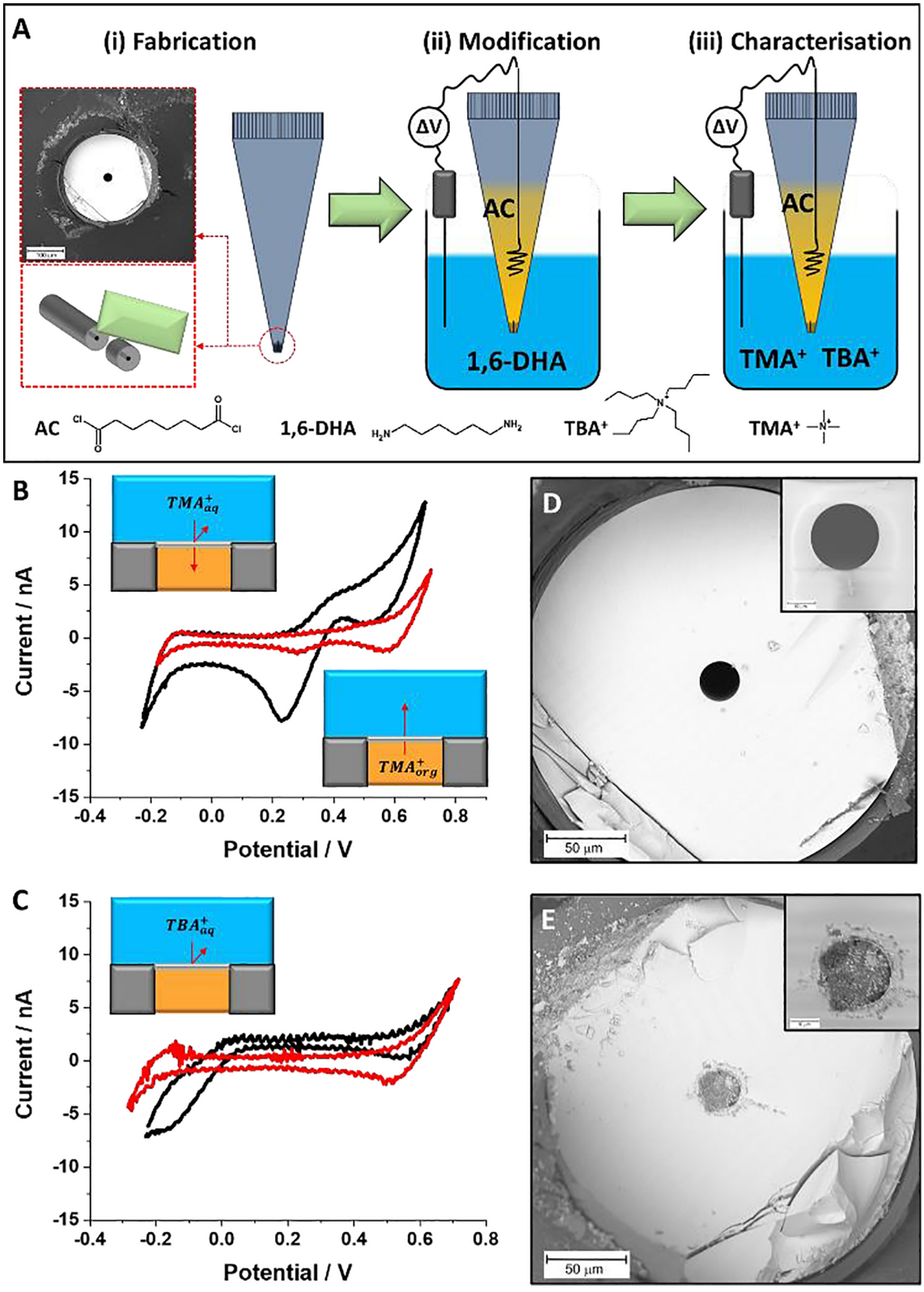

Fig. 3. A – A schematic representation of an experimental protocol involving (i) fabrication of a microscopic ITIES (supported with a piece of silica capillary tubing; the SEM photo shows the capillary embedded in plastic casing), (ii) electrochemical modification of the microscopic ITIES with nylon-6,6; (iii) electrochemical characterization of the modified microscopic ITIES in the presence of TMA^+ and TBA^+. The ITVs show the currents corresponding to the TMA^+ (**B**) and TBA^+ (**C**) initially present in the aqueous phase before and after modification. **D** and **E** (also insets) show SEM micrographics of a fused silica microcapillary before and after modification, respectively.

1,6-DAM^{2+}). A further increase in pH, especially in the pH range from 9 to 13, causes significant fluctuations in the fraction of non- (1,6-DAH^{0}), mono- (1,6-DAM^{+}) and 1,6-DAH^{2+} species. This is also reflected in the position and intensity of the positive and negative peaks attributed to 1,6-DAH ion transfer (see ITVs in Fig. S3). The tentative rule says that the potential of ion transfer can be directly attributed to the hydrophilicity of the molecule under investigation. That is, more hydrophilic cations require a higher portion of the potential applied to the LLI to trigger their interfacial transfer [36]. Consequently, as the concentration of 1,6-DAH^{+} and 1,6-DAH^{0} species (both being slightly more hydrophobic than 1,6-DAH^{2+}) increase, we have observed dropping peak currents and a shift in the transfer potential towards lower potential values. For further experiments involving interfacial polycondensation of nylon-6,6 we have fixed the pH of the aqueous phase at 12, under which conditions 1,6-DAH species exist as the 1,6-DAH^{0} and 1,6-DAH^{+} species in a ratio of about 1:1. A pH optimization study was performed and is summarized in Section 2.4 of the Supporting information. Fig. 2A shows a series of cyclic voltammograms recorded with 5 mM 1,6-DAH in the water phase, 5 mM AC in the organic phase and with both reagents at 5 mM concentration in both the water and the organic phases. Without a permanent charge or ionizable chemical functional group, the AC is electrochemically inactive. The product of its hydrolysis, adipic acid, although probably formed, does not give a signal within the available potential window (ITVs recorded with and without 5 mM AC in the organic phase with the pH of the aqueous phase set to 2 and 12 revealed no differences). A clear signal appears when only 5 mM 1,6-DAH was present in the aqueous phase – Fig. 2A, blue dotted curve. In this particular case, the positive current limiting the potential widow starts increasing 195 mV earlier than the blank and originates from 1,6-DAH^{+} transfer from the water to the organic phase. Further positive polarization eventually triggers Na^{+} transfer from the water to the organic phase. The most interesting situation occurs when both reagents are present in the biphasic system, i.e. 1,6-DAH in the water and AC in the organic phase. First of all, the point at which the positive current starts increasing is further shifted to lower potential values by around 80 mV. Moreover, after just one voltammetric cycle film can be clearly seen with the naked eye at the soft junction (see the photo in the top right-hand corner of Fig. 2B). The material formed at the ITIES contained several absorption bands characteristic of polyamides, as shown using infra-red spectrometry (for details see Section 2.5 in the Supporting information). The blank experiment set in a beaker revealed that for identical conditions but without external polarization, nylon-6,6 film is again formed, but requires more time (2–3 min). The proposed mechanism of electrochemically controlled nylon-6,6 interfacial polymerization is shown schematically in Fig. 2B. Here a number of mutually interconnected reactions can occur. First of all, (i) the 1,6-DAH^{0} can react with AC within the interfacial region giving polyamide and hydrochloric acid which dissociates into H^{+} and Cl^{-}. As the interface is polarized using an external power source, (ii) H^{+} may be transferred to either the organic or the aqueous phase. In the latter case, especially within the interfacial region, (iii) the amine groups of the 1,6-DAH^{0} will be protonated, and hence, the resulting cations may undergo an interfacial ion transfer reaction. (iv) We cannot exclude protonated amine dissociation, especially in the mixed layer region, giving rise to non-protonated amine groups available for reaction with the acyl chloride functional groups and (v) H^{+} further acidifying the aqueous phase layer adjacent to the LLI. All these reactions lead to the formation of a probably partially positively-charged polyamide film that may find applications in size- and charge-sieving-based molecular separation.

To demonstrate the applicability of the developed procedure, we have used electrochemical control to modify the microscopic LLI with nylon-6,6 based films. Firstly, we prepared the microITIES using fused silica capillaries with an internal diameter equal to 25 μm (the protocol of microITIES preparation is described elsewhere) [37]. Electrochemical studies revealed that the location of the ITIES is at the pore ingress and the diameter of the ITIES of 23.2 μm (see Supporting information Section 2.6) agrees very well with the pore diameter measured using SEM (24.8 μm – Fig. 3D). The protocol for the modification of the microITIES with nylon-6,6 is depicted in Fig. 3A. Briefly, the freshly prepared capillaries were filled with the organic phase containing 5 mM AC. Next, these were immersed in a water phase containing 5 mM 1,6-DAH. The electrodes and connections were fixed and five voltammetric cycles were recorded. The SEM micrographs clearly show that a deposit is present within the pore after the electrochemical modification process (Fig. 3E), unlike the unmodified pore (Fig. 3D).

Next, the modified capillary was placed directly into a cell containing either tetramethylammonium (TMA^{+}) or tetrabutylammonium (TBA^{+}) cations. Fig. 3B and C show the ITVs recorded before and after modification in the presence of the specified quaternary ammonium cations in the water phase at a concentration equal to 60 μM. It is nicely shown that the transfer of TBA^{+} is entirely blocked (signal appearing on the negative side of the potential window in Fig. 3C) whereas the faradaic current for TMA^{+} is reduced by 90%. The proposed platform combines a very simple LLI miniaturization approach with an ITIES modification protocol which is equally straightforward. As a whole, the proposed configuration may find applications in sensing, selected molecular recovery or separation.

4. Conclusions

In this work we have shown that the interfacial deposition of polyamide based films can be controlled using electrochemically triggered ion transfer. Precise control of the pH is essential in this respect, as protonation of the amine groups within 1,6-DAH inhibits the reaction with the AC. The resulting polyamide films can be easily removed from the interface, which is of the utmost importance for practical applications. Additionally, micropores with a diameter of 25 μm were used to support the polarized LLI and were further modified under electrochemical control with the polyamide film. The resulting platform exhibited size-sieving properties, being partially permeable to tetramethylammonium cations and entirely inhibiting the interfacial transport of the tetrabutylammonium cation.

Conflicts of interest

There are no conflicts to declare.

CRediT authorship contribution statement

Karolina Kowalewska: Investigation, Formal analysis. **Karolina Sipa:** Investigation, Formal analysis. **Andrzej Leniart:** Investigation, Formal analysis. **Sławomira Skrzypek:** Supervision, Writing - review & editing. **Lukasz Poltorak:** Methodology, Visualization, Supervision, Project administration, Funding acquisition, Writing - review & editing, Writing - original draft.

Acknowledgments

This project was financially supported by the National Science Center (NCN) in Krakow, Poland (Grant no. UMO-2018/31/D/ST4/03259).

Appendix A. Supplementary data

Supplementary data to this article can be found online at https://doi.org/10.1016/j.elecom.2020.106732.

References

[1] L. Poltorak, A. Gamero-Quijano, G. Herzog, A. Walcarius, Decorating soft electrified interfaces: from molecular assemblies to nano-objects, Appl. Mater. Today 9 (2017)

533–550, https://doi.org/10.1016/j.apmt.2017.10.001.
[2] K. Piradashvili, E.M. Alexandrino, F.R. Wurm, K. Landfester, Reactions and polymerizations at the liquid–liquid interface, Chem. Rev. 116 (2016) 2141–2169, https://doi.org/10.1021/acs.chemrev.5b00567.
[3] W.H. Carothers, Linear Polyamides and their Production, US Patent US2130523A, 1938.
[4] R. Roux, L. Sallet, P. Alcouffe, S. Chambert, N. Sintes-Zydowicz, E. Fleury, J. Bernard, Facile and rapid access to glyconanocapsules by CuAAC interfacial polyaddition in miniemulsion conditions, ACS Macro Lett. 1 (2012) 1074–1078, https://doi.org/10.1021/mz300281u.
[5] C.K. Chen, Q. Wang, C.H. Jones, Y. Yu, H. Zhang, W.C. Law, C.K. Lai, Q. Zeng, P.N. Prasad, B.A. Pfeifer, C. Cheng, Synthesis of pH-responsive chitosan nanocapsules for the controlled delivery of doxorubicin, Langmuir 30 (2014) 4111–4119, https://doi.org/10.1021/la4040485.
[6] N. Anton, J.P. Benoit, P. Saulnier, Design and production of nanoparticles formulated from nano-emulsion templates – a review, J. Control. Release 128 (2008) 185–199, https://doi.org/10.1016/j.jconrel.2008.02.007.
[7] G.T. Vladisavljević, R.A. Williams, Recent developments in manufacturing emulsions and particulate products using membranes, Adv. Colloid Interface Sci. 113 (2005) 1–20, https://doi.org/10.1016/j.cis.2004.10.002.
[8] S.Y. Teh, R. Lin, L.H. Hung, A.P. Lee, Droplet microfluidics, Lab. Chip 8 (2008) 198–220, https://doi.org/10.1039/b715524g.
[9] M. Sairi, J. Strutwolf, R.A. Mitchell, D.S. Silvester, D.W.M. Arrigan, Chronoamperometric response at nanoscale liquid–liquid interface arrays, Electrochim. Acta 101 (2013) 177–185, https://doi.org/10.1016/j.electacta.2012.11.062.
[10] Y.H. Lanyon, G. De Marzi, Y.E. Watson, A.J. Quinn, J.P. Gleeson, G. Redmond, D.W.M. Arrigan, Fabrication of nanopore array electrodes by focused ion beam milling, Anal. Chem. 79 (2007) 3048–3055, https://doi.org/10.1021/ac061878x.
[11] M.D. Scanlon, J. Strutwolf, A. Blake, D. Iacopino, A.J. Quinn, D.W.M. Arrigan, Ion-transfer electrochemistry at arrays of nanointerfaces between immiscible electrolyte solutions confined within silicon nitride nanopore membranes, Anal. Chem. 82 (2010) 6115–6123, https://doi.org/10.1021/ac1008282.
[12] R. Zazpe, C. Hibert, J. O'Brien, Y.H. Lanyon, D.W.M. Arrigan, Ion-transfer voltammetry at silicon membrane-based arrays of micro-liquid-liquid interfaces, Lab. Chip 7 (2007) 1732–1737, https://doi.org/10.1039/b712601h.
[13] E. Bak, M. Donten, M. Skompska, Z. Stojek, Electrodeposition of poly(N-vinylcarbazole) at the three-phase junction. Formation of very different polymer structures, J. Phys. Chem. B 110 (2006) 24635–24641, https://doi.org/10.1021/jp063935w.
[14] M. Li, H. Zhu, X. Mao, W. Xiao, D. Wang, Electropolymerization of polypyrrole at the three-phase interline: influence of polymerization conditions, Electrochim. Acta 92 (2013) 108–116, https://doi.org/10.1016/j.electacta.2013.01.016.
[15] I. Kaminska, M. Jonsson-Niedziolka, A. Kaminska, M. Pisarek, R. Hołys, M. Opallo, J. Niedziolka-Jonsson, Electrodeposition of well-adhered multifarious Au particles at a solid|toluene|aqueous electrolyte three-phase junction, J. Phys. Chem. C 116 (2012) 22476–22485, https://doi.org/10.1021/jp307674k.
[16] J. Niedziolka, M. Opallo, Electrochemically assisted sol–gel process at a three phase junction, Electrochem. Commun. 10 (2008) 1445–1447, https://doi.org/10.1016/j.elecom.2008.07.039.
[17] V. Lakshminarayanan, L. Poltorak, D. Bosma, E.J.R. Sudhölter, J.H. van Esch, E. Mendes, Locally pH controlled and directed growth of supramolecular gel microshapes using electrocatalytic nanoparticles, Chem. Commun. 55 (2019) 9092–9095, https://doi.org/10.1039/c9cc04238e.
[18] L. Poltorak, G.G. Herzog, A. Walcarius, Electrochemically assisted generation of silica deposits using a surfactant template at liquid/liquid microinterfaces, Langmuir 30 (2014) 11453–11463, https://doi.org/10.1021/la501938g.
[19] L. Poltorak, K. Morakchi, G. Herzog, A. Walcarius, Electrochemical characterization of liquid-liquid micro-interfaces modified with mesoporous silica, Electrochim. Acta 179 (2015) 9–15, https://doi.org/10.1016/j.electacta.2015.01.129.
[20] L. Poltorak, M. Hébrant, M. Afsharian, M. Etienne, G. Herzog, A. Walcarius, Local pH changes triggered by photoelectrochemistry for silica condensation at the liquid-liquid interface, Electrochim. Acta 188 (2016) 71–77, https://doi.org/10.1016/j.electacta.2015.11.107.
[21] A. Holzinger, G. Neusser, B.J.J. Austen, A. Gamero-Quijano, G. Herzog, D.W.M. Arrigan, A. Ziegler, P. Walther, C. Kranz, Investigation of modified nanopore arrays using FIB/SEM tomography, Faraday Discuss. 210 (2018) 113–130, https://doi.org/10.1039/c8fd00019k.
[22] L. Poltorak, N. van der Meijden, S. Oonk, E.J.R. Sudhölter, M. de Puit, Acid phosphatase behaviour at an electrified soft junction and its interfacial co-deposition with silica, Electrochem. Commun. 94 (2018) 27–30, https://doi.org/10.1016/j.elecom.2018.07.022.
[23] G. Herzog, V. Kam, D.W.M. Arrigan, Electrochemical behaviour of haemoglobin at the liquid/liquid interface, Electrochim. Acta 53 (2008) 7204–7209, https://doi.org/10.1016/j.electacta.2008.04.072.
[24] E. Alvarez de Eulate, S. O'Sullivan, D.W.M. Arrigan, Electrochemically induced formation of cytochrome C oligomers at soft interfaces, ChemElectroChem 4 (2017) 898–904, https://doi.org/10.1002/celc.201600851.
[25] G. Herzog, S. Flynn, C. Johnson, D.W.M. Arrigan, Electroanalytical behavior of poly-L-lysine dendrigrafts at the interface between two immiscible electrolyte solutions, Anal. Chem. 84 (2012) 5693–5699.
[26] A. Berduque, M.D. Scanlon, C.J. Collins, D.W.M. Arrigan, Electrochemistry of non-redox-active poly(propylenimine) and poly(amidoamine) dendrimers at liquid-liquid interfaces, Langmuir 23 (2007) 7356–7364, https://doi.org/10.1021/la063294w.
[27] P.S. Toth, A.N.J. Rodgers, A.K. Rabiu, R.A.W. Dryfe, Electrochemical activity and metal deposition using few-layer graphene and carbon nanotubes assembled at the liquid–liquid interface, Electrochem. Commun. 50 (2015) 6–10, https://doi.org/10.1016/j.elecom.2014.10.010.
[28] Y. Li, O. Zaluzhna, Y.J. Tong, Identification of a source of size polydispersity and its solution in Brust-Schiffrin metal nanoparticle synthesis, Chem. Commun. 47 (2011) 6033–6035, https://doi.org/10.1039/c1cc11642h.
[29] Y. Li, O. Zaluzhna, B. Xu, Y. Gao, J.M. Modest, Y.Y.J. Tong, Mechanistic insights into the Brust-Schiffrin two-phase synthesis of organo-chalcogenate-protected metal nanoparticles, J. Am. Chem. Soc. 133 (2011) 2092–2095, https://doi.org/10.1021/ja1105078.
[30] M. Platt, R.A.W. Dryfe, Structural and electrochemical characterisation of Pt and Pd nanoparticles electrodeposited at the liquid/liquid interface: Part 2, Phys. Chem. Chem. Phys. 7 (2005) 1807–1814 http://www.ncbi.nlm.nih.gov/pubmed/19787942.
[31] U. Evans-Kennedy, J. Clohessy, V.J. Cunnane, Spectroelectrochemical study of 2,2':5',2''-terthiophene polymerization at a liquid / liquid interface controlled by potential-determining ions, Macromolecules 37 (2004) 3630–3634.
[32] P.S. Toth, A.K. Rabiu, R.A.W. Dryfe, Controlled preparation of carbon nanotube-conducting polymer composites at the polarisable organic/water interface, Electrochem. Commun. 60 (2015) 153–157, https://doi.org/10.1016/j.elecom.2015.08.022.
[33] K. Maeda, H. Jänchenová, A. Lhotský, I. Stibor, J. Budka, V. Mareček, Formation of a polymer layer from monomers adsorbed at a liquid | liquid interface, J. Electroanal. Chem. 516 (2001) 103–109, https://doi.org/10.1016/S0022-0728(01)00658-1.
[34] B. Li, Y. Qiao, J. Gu, X. Zhu, X. Yin, Q. Li, Z. Zhu, M. Li, P. Jing, Y. Shao, Electrochemical behaviors of protonated diamines at the micro-water/1,2-dichloroethane interface, J. Electroanal. Chem. 726 (2014) 21–26, https://doi.org/10.1016/j.jelechem.2014.05.007.
[35] D.R. Lide, CRC Handbook of Chemistry and Physics, 84th Edition, 53 (2003) 2616.
[36] A.J. Olaya, M.A. Méndez, F. Cortes-Salazar, H.H. Girault, Voltammetric determination of extreme standard Gibbs ion transfer energy, J. Electroanal. Chem. 644 (2010) 60–66, https://doi.org/10.1016/j.jelechem.2010.03.030.
[37] K. Rudnicki, L. Poltorak, S. Skrzypek, E.J.R. Sudhölter, Fused silica micro-capillaries used for a simple miniaturization of the electrified liquid – liquid interface, Anal. Chem. 90 (2018) 7112–7116, https://doi.org/10.1021/acs.analchem.8b01351.